SPECTROSCOPIC INVESTIGATIONS

OF THE BETA-AMYLOID PEPTIDE

A Thesis

Presented to the Faculty of the Graduate School

at the University of Missouri – Columbia

In Partial Fulfillment of the Requirements for the Degree

Master of Science

By

EMILY ANN SCHMIDT

Dr. Renee Jiji, Thesis Supervisor

AUGUST 2008

The undersigned, appointed by the dean of the Graduate School, have examined the thesis entitled

SPECTROSCOPIC INVESTIGATIONS OF THE BETA-AMYLOID PEPTIDE

presented by Emily Ann Schmidt,

a candidate for the degree of Master of Science, and hereby certify that, in their opinion, it is worthy of acceptance.

_____

Professor Renee Jiji

_____

Professor Sheryl Tucker

_____

Professor Shi-Jie Chen

ACKNOWLEDGEMENTS

I would like to thank my advisor, Dr. Renee Jiji, for her patience and guidance with my research. I would also like to thank my group members for their support. I want to acknowledge Dr. Mike Henzl for his help with the CD measurements, to Dr. Fabio Gallazzi for synthesizing the crude Aβ(1-40) used in this study, and to Dr. Nathan Leigh for the MS analysis. I would also like to acknowledge the Experiment Station Chemical Laboratories at the University of Missouri – Columbia for performing the AAA analysis. Finally, I would like to thank the Department of Chemistry at the University of Missouri – Columbia for funding.

TABLE OF CONTENTS

LIST OF FIGURES

LIST OF TABLES

ABSTRACT

The focus of this project is two-fold: examining the native structures of three different fragments of the beta-amyloid (Aβ) peptide, and attempting to overcome some of the difficulties encountered in such an examination. The first part uses two different spectroscopic methods to compare the native structures of the hydrophilic Aβ(1-16) fragment, the hydrophobic Aβ(25-40) fragment, and the longer Aβ(1-40) fragment. The second part focuses on replacing the counter-ion used in peptide purifications, including the purification of the Aβ peptide, with a counter-ion that is less likely to alter the secondary structure and will not interfere with vibration-based spectroscopic studies. The third part highlights an attempt to improve upon current methods of peptide concentration estimation. Many experimental measurements require an accurate estimate of peptide concentration, which can prove to be particularly problematic for peptides such as Aβ that are not easily soluble in aqueous solvents.

CHAPTER 1:

Comparison of the Steady State Structure of Three Different Fragments of the Beta-Amyloid Peptide

1.1 Introduction

The beta-amyloid peptide (Aβ) is the primary component of the plaques found in the brains of patients with Alzheimer's disease.[1, 2] While it is still unclear whether Alzheimer's disease causes or is caused by the presence of the plaques in the brain, the beta-amyloid peptide is involved.[1, 3] Understanding the native structure of this peptide could provide insight as to why some proteins are more prone to fibrillization.

Research has shown that the Aβ peptide forms from the amyloid precursor protein (APP).[4] The Aβ peptide is formed when APP is cleaved first by a β-secretase at the N-terminus of what will be the Aβ peptide, and then cleaved by a γ-secretase deep within the membrane at the C-terminus of the Aβ peptide.[4] The Aβ peptide is typically 40 or 42 amino acid residues in length. Aβ(1-40) is the most common length found in the body, but Aβ(1-42) aggregates the most aggressively, and is the primary component of the plaques found in the brain of Alzheimer's patients.[1]

Three different lengths of the beta-amyloid peptide were used in this study: Aβ(1-16), Aβ(25-40), and Aβ(1-40). The amino acid sequence of Aβ(1-40) is:

DAEFRHDSGYEVHHQKLVFFAEDV***GSNKGAIIGLMVGGVV***

The first highlighted portion of the sequence above is Aβ(1-16), and the second highlighted portion is Aβ(25-40). The Aβ(1-16) fragment represents the most hydrophilic

portion of the full Aβ peptide, and is typically considered to display polyproline II, or PPII-type, conformation in aqueous solvents.[5] PPII has replaced previous terminology that grouped the extended structures in with more disordered conformations under the misnomer of "random coil".[6] PPII type structure is neither random nor α-helical.[6] (Figure 1.1) The Aβ(25-40) fragment is the most hydrophobic, and the conformation is a combination of β-strand and some PPII structure, but more disordered than Aβ(1-16).[5]

Given that Aβ(1-42) is more prone to aggregation, Aβ(1-40) was used in these studies.[3] Aβ(1-40) is a reasonable analogue for the full-length Aβ(1-42) peptide because it also forms fibrils, though at a much slower rate.[3]

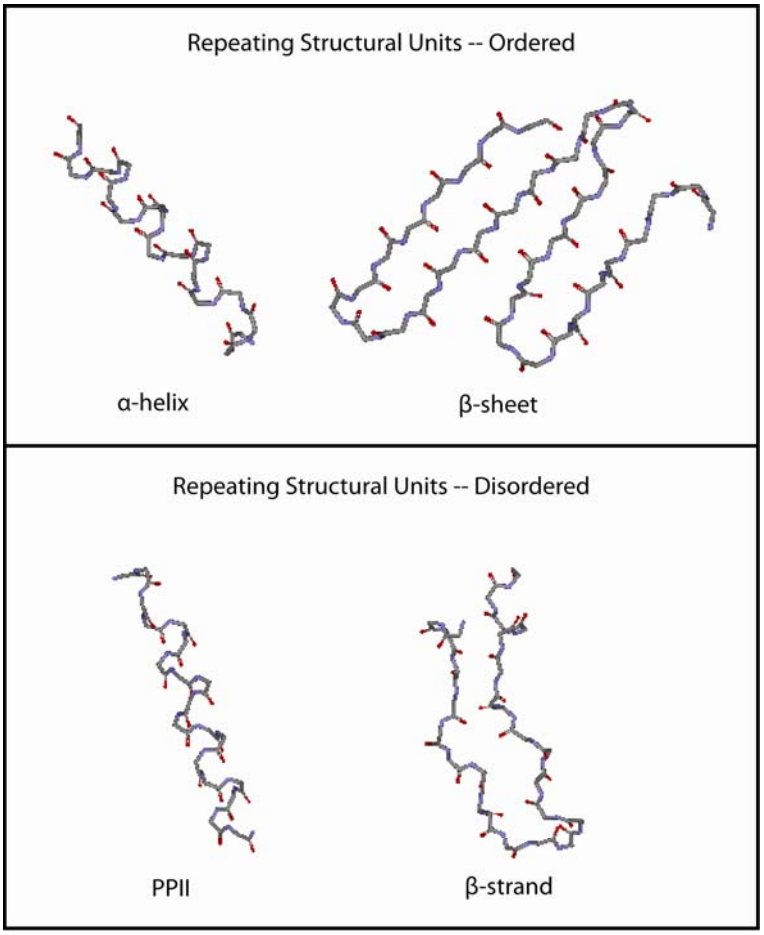

Figure 1.1 Structural representations of four different types of secondary structure

1.2 Theory

Circular Dichroism Spectroscopy. Circular dichroism (CD) occurs when right-handed and left-handed circularly polarized light are differentially absorbed by a molecule.[7] In a symmetrical molecule, there will be no difference in the absorbance between the right and left circularly polarized light, but in asymmetrical molecules that display some type of structure, there will be a measurable difference in the absorbance.

$$\Delta A = A_L - A_R \qquad \text{(Eq. 1.1)}$$

Even though what are actually measured are the absorbance values for both the right (A_R) and left (A_L) circularly polarized light and the difference (ΔA) is calculated, that is not the value typically recorded. The ΔA value is first converted to the ellipticity (θ) in degrees.[7]

$$\theta = 2.303 * \Delta A * \frac{180}{4\pi} \qquad \text{(Eq. 1.2)}$$

Because of historical precedents, the ellipticity is further converted to mean residue ellipticity (θ_{MRE}), with units of deg cm^2 dmol^{-1}, where M is molecular weight (g/mol), c is concentration (g/cm^3), l is the path length of the cell (cm), and n_r is the number of amino acid residues.[7]

$$\theta_{MRE} = \frac{\theta}{10} * \frac{M}{c * l * n_r} \qquad \text{(Eq. 1.3)}$$

In the UV region particularly, information about protein secondary structure can be found in CD spectra.[6, 8] (Figure 1.2) Because CD is inherently an absorbance measurement, the reported spectrum will actually be a sum of the absorbance for each structural type found in the molecule. It is possible to estimate the percentage concentration of each structural type in the protein based on the CD spectrum, but it is not as accurate as x-ray crystallography, for instance.[7]

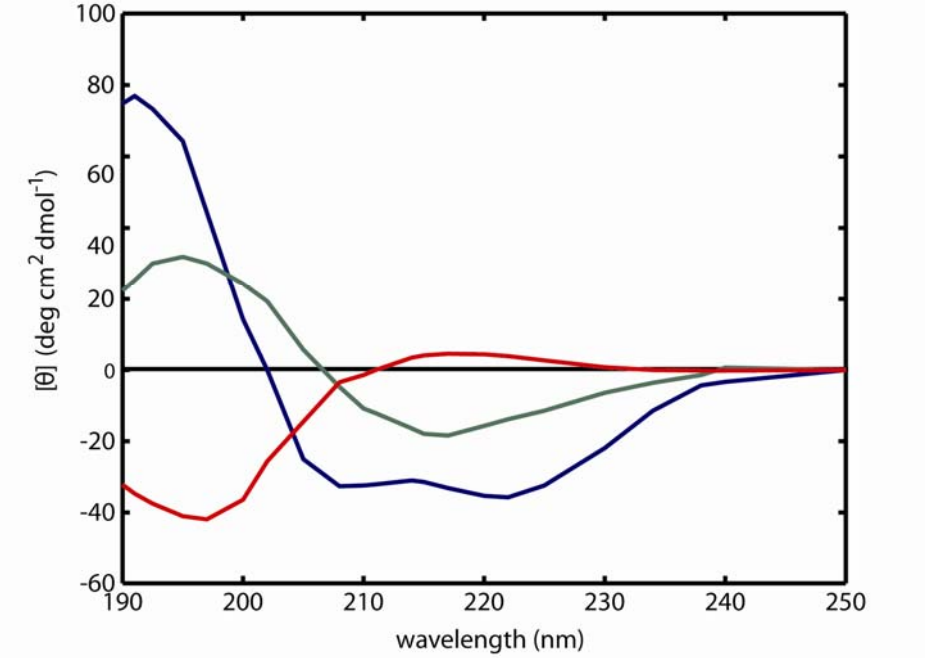

Figure 1.2 Representative CD spectra of poly-L-lysine in three distinct, pure protein structural conformations are a) —— α-helix, b) —— β-sheet, and c) —— PPII. (Recreated from Greenfield and Fasman, *Biochem* **1969**, *8(10)*, 4108-4116)

UV Resonance Raman Spectroscopy. UV resonance Raman (UVRR) is an experimental technique that allows for examination of the vibrational frequencies particular to the various bonds within a molecule, or in this case, the beta-amyloid peptide.[7, 9] Raman scattering is a light-scattering phenomenon similar to Rayleigh scattering. Rayleigh scattering is elastic, meaning no energy is transferred between the incoming light and the molecule, and the frequency of the incoming light is the same as the frequency of the scattered light. In Raman scattering, the interaction between the light and molecule is inelastic; there is a change in frequency of the scattered light versus the incoming light, and this energy change corresponds to the vibrational energy of a particular bond within the molecule.[7, 9, 10]

With Raman scattering, when the incoming light is absorbed by the molecule, the molecule is promoted to a virtual excited state, below an actual electronic transition.[7, 9, 10] As the molecule relaxes, it returns to a vibrational level at either +1 (Stokes) or -1 (anti-Stokes) of the initial vibrational state.[7, 9, 10] The Raman scattering intensity is also dependent upon the polarizability of the molecule – the greater the polarizability, the greater the Raman scattering.[7, 9, 10] Even so, the overall intensity of the Raman scattering is extremely low relative to the initial light intensity, or even Rayleigh scattering.[9]

The signal intensity of the Raman scattering can be dramatically increased through resonance-enhancement of the vibrations. This occurs when the molecule is promoted to a virtual state after undergoing an electronic transition. Resonance enhancement increases the signal intensity because the molecular polarizability is increased by a power of four.[7, 9, 10]

Particular vibrations in each bond in the molecule will change the energy of the scattered light to a different extent. There are four regions of the UVRR spectra that are of particular interest in peptide studies referred to as the amide I, II, III, and S regions. The amide I region is typically located between 1650 and 1680 cm^{-1} and represents C=O stretching.[10-12] The amide II region is found between 1500 and 1600 cm^{-1} and the amide III region is between 1200 and 1350 cm^{-1}. The amide II is an in-phase and amide III is an out-of-phase combination of N-H in-plane bending and C-N stretching.[10-12] The amide S band is near 1400 cm^{-1} and involves C_{α}-H bending.[11-13]

Actual band assignments vary depending upon how much of each structural type (α-helix, β-sheet, etc.) is present in the molecule. The amide I bands tend to be shifted to lower frequencies with higher α-helical content.[11, 14] The amide II and S band areas and

intensities will decrease with an increase in α-helical content, though the band positions remain relatively unchanged.[15] The amide III bands will shift to higher frequencies with increasing α-helical content.[11]

1.3 Experimental

1.3.1 Materials

The Aβ(1-16) and Aβ(25-40) peptide fragments were purchased from Global Peptide (Fort Collins, CO) and used without further purification (96% purity). Aβ(1-40) was purchased from Biopeptide (San Diego, CA) and used without further purification (>95% purity). The phosphate buffer was prepared from sodium phosphate monobasic and sodium phosphate dibasic, both of which were purchased from Fisher (Pittsburgh, PA). HPLC grade hydrochloric acid (HCl) and ammonium hydroxide (NH_4OH) were also purchased from Fisher. Sodium perchlorate was purchased at Acros Organics (Geel, Belgium).

1.3.2 Sample Preparation

Circular Dichroism. Solutions of Aβ(1-16) and Aβ(25-40) were prepared by first dissolving ~0.2 mg of peptide in 100 μL of 10 mM NH_4OH and diluting to 1.0 mL with 10 mM phosphate buffer (pH 7.4).

UV Resonance Raman. Each of the Aβ peptide fragment samples used for this study was prepared by dissolving ~1.5 mg of peptide into 300 μL of 10 mM NH_4OH and diluting to 5.0 mL with 10 mM phosphate buffer (pH 7.4). Sodium perchlorate was then

added. The final concentrations for each Aβ solution were approximately 30 mM Aβ and 50 mM perchlorate in 10 mM phosphate buffer.

1.3.3 Measurements

Circular Dichroism. Measurements were made using 0.1 cm quartz cuvettes (Hellma, Plainview, NY) with an Aviv 62DS CD spectrometer (Lakewood, NJ). Settings were held at a constant temperature of 4°C scanning from 250 to 190 nm over 5 minutes. Data collection was repeated five times.

UV Resonance Raman. All measurements were made using a tunable Ti-sapphire laser (Coherent Evolution, Santa Clara, CA) with a Spex 1250M monochromator and a Symphony CCD detector (Horiba-Jobin Yvon, Edison, NJ). The laser was set for 195 nm excitation and data collected in 30 second increments for a total of 80 cycles, or 200 minutes (~3.5 hours).

1.3.4 Data Analysis

Circular Dichroism. The data was processed using MatLab (MathWorks, Natick, MA). All spectra were averaged and blank-corrected before converting the collected ΔA values to mean residue ellipticity by the calculations as described above. The curves were then fit using a smoothing spline algorithm in the CurveFit Toolbox in MatLab.

UV Resonance Raman. The data was processed using MatLab (MathWorks, Natick, MA). The spectra were averaged together, and any cosmic spikes were removed using a cosmic ray removal program written in the lab. A blank spectrum was used to

remove the contribution of the water band from each sample spectrum. A non-linear least squares algorithm, also written in the lab, was then used to deconvolute the spectra.

1.4 Results & Discussion

Circular Dichroism. The CD spectra for Aβ(1-16) and Aβ(25-40) are quite distinct from one another as might be expected because of the marked differences between the two peptide fragments. As mentioned earlier, the Aβ(1-16) fragment is the more hydrophilic fragment and is considered to display PPII-like structure, which is consistent with the data collected here.[6] (Figure 1.3) The Aβ(25-40) fragment is more hydrophobic and contains a mixture of β-strand and other disordered conformations. This assumption is also consistent with the data collected. (Figure 1.4) The CD spectrum for Aβ(1-40) looks remarkably similar in shape to the Aβ(25-40) spectrum, implying that it is predominantly disordered in nature under these experimental conditions. (Figure 1.5)

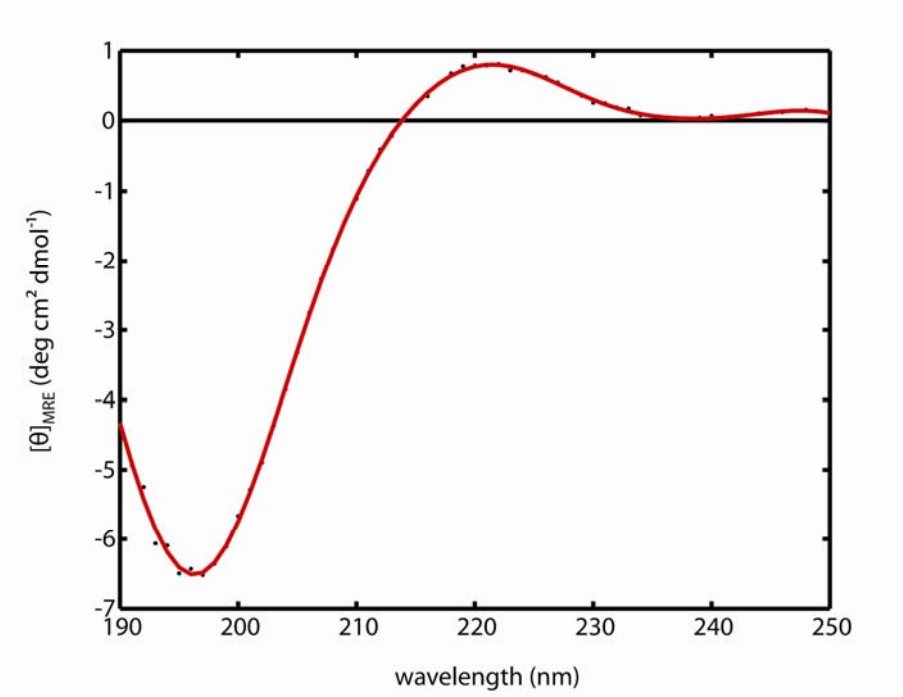

Figure 1.3 CD spectrum of Aβ(1-16) collected at 4°C and pH 7.4.

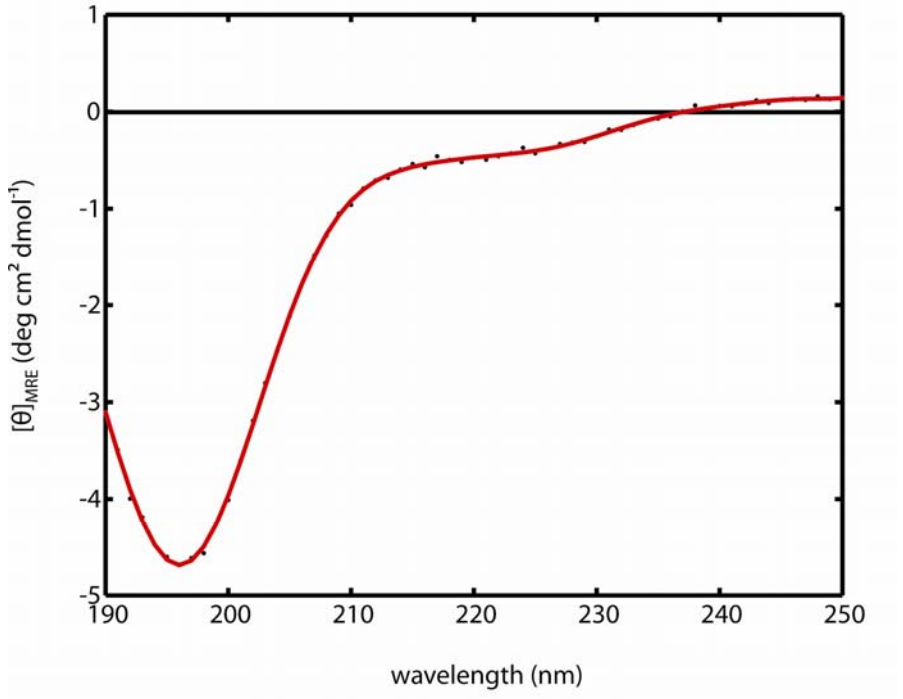

Figure 1.4 CD spectrum of Aβ(25-40) collected at 4°C and pH 7.4.

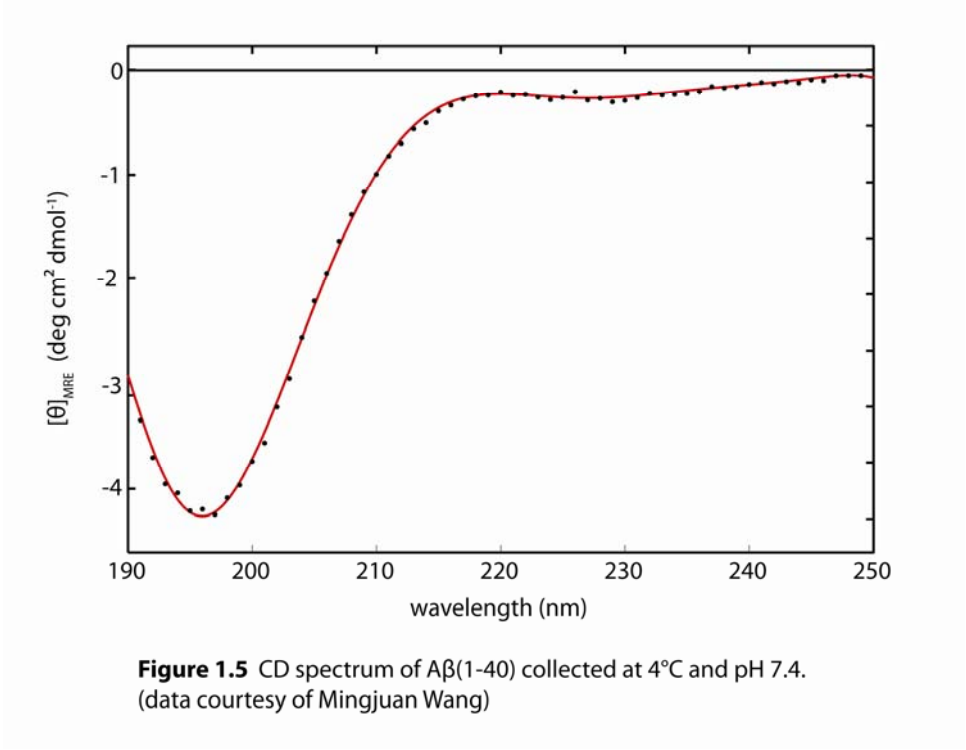

Figure 1.5 CD spectrum of Aβ(1-40) collected at 4°C and pH 7.4. (data courtesy of Mingjuan Wang)

UV Resonance Raman. The UVRR spectrum of Aβ(1-16) fragment is in fact consistent with previous work suggesting that it contains a high level of PPII conformation. Other workers have shown that peptides containing significant amounts of PPII will display fewer bands in the amide III region, with a relatively strong, broad band near 1250 cm^{-1}, consistent with the spectrum presented in Figure 1.6.[12, 16] However, tyrosine has a band at ~1260 cm^{-1} that may be contributing to the strong intensity of the band at 1261 cm^{-1}. There are two bands in the amide I region at 1642 and 1680 cm^{-1}. The ratio of the amide I bands, 1642 and 1680 cm^{-1}, is nearly 1:2. In the UVRR spectra of the other two fragments, the intensity of the band at ~1680 cm^{-1} is much greater when compared to the band at ~1640 cm^{-1}. This may mean that a decrease in the intensity of the band at 1640 cm^{-1} with an increase in intensity of the band at 1680 cm^{-1} corresponds to an overall decrease in the content of PPII-type structure.

The UVRR spectrum of Aβ(25-40) should show more characteristics of a combination of β-strand, PPII, and disordered conformations. The spectrum does indeed seem to support this premise. (Figure 1.7) There are additional amide III region bands present in the Aβ(25-40) spectrum, and the band widths and intensities are more evenly distributed than the amide III region bands of Aβ(1-16). If the ratio of relative band intensities of the amide I modes at ~1645 and 1680 cm^{-1} is indicative of the level of PPII structure, this also supports the idea that the Aβ(25-40) peptide should contain significantly less PPII structure than Aβ(1-16). The ratio between the two bands is closer to 1:4. It is also important to note that there are no aromatic residues present in the Aβ(25-40) fragment that could potentially affect the position and strength of the amide I band at 1648 cm^{-1}, as there are in both the Aβ(1-16) and Aβ(1-40) peptide fragments. This means that the close ratio of the two amide I bands in the Aβ(1-16) fragment may be that much more remarkable.

Aβ(1-40) should theoretically be some combination of both the Aβ(1-16) and Aβ(25-40) peptide conformations, and that holds true in the Aβ (1-40) UVRR spectrum. (Figure 1.8) As with the Aβ(25-40) spectrum, the amide III bands are relatively broad and equal in intensity. However, as in the Aβ(1-16) spectrum, bands corresponding to tyrosine and phenylalanine are also present, and more intense because there are three phenylalanine residues to the one tyrosine residue in the Aβ(1-40) peptide fragment. This may be why the band at ~1645 cm^{-1} is no longer visible in the Aβ(1-40) spectrum; the intensities of the combined phenylalanine and tyrosine residues at 1590 and 1616 cm^{-1} could potentially be overwhelming the presence of the second amide I mode. The absence

of that mode may also point to an even lower content of PPII relative to the overall structure than is present in either of the other fragments.

Another interesting feature regarding the Aβ(1-40) spectrum is that several of the amide modes correlate very well to values suggestive of β-sheet structure.[12] Formation of β-sheets could be a possibility because a solely monomeric population of Aβ(1-40) peptide fragments was not established for this experiment. It is also possible to display some β-sheet characteristics with a wholly monomeric population because the Aβ(1-40) peptide is long enough to be able to form intramolecular H-bonds.

1.5 Conclusion

There are distinct spectroscopic differences between the Aβ(1-16) and Aβ(25-40) peptide fragments. Both CD and UVRR confirm that Aβ(1-16) has more PPII structure than the more disordered Aβ(25-40), consistent with hydrophilic and hydrophobic properties, respectively. Though the data presented suggests that the Aβ(1-40) peptide represents a mixture of the conformations of the two smaller fragments, it also supports the idea that the Aβ(1-40) fragment contains some additional β-sheet structure.

Table 1.1 UVRR band assignments* at 195 nm excitation			
	Shift (cm^{-1})		
	Aβ(1-16)	**Aβ(25-40)**	**Aβ(1-40)**
ClO_4^-	934	934	934
Phe	1004	-	1003
Phe	1033	-	1031
PO_4^-	1095	1095	1079
Tyr/Phe	1181	-	1183
Tyr/Phe	1209		1209
amide III	-	1219	-
	-	1248	1241
	1261**	1278	1268
	1312	1313	1310
	1341	1345	1346
amide S	1397	1392	1395
TFA	1440	1441	1441
amide II	1537	1528	1519
	1562	1564	1562
Tyr/Phe	1607	-	1590
Tyr/Phe	1623	-	1616
amide I	1642	1648	-
	1680	1680	1676

(*): full band assignment parameters in appendix
(**): most likely a combination of amide III and Tyr

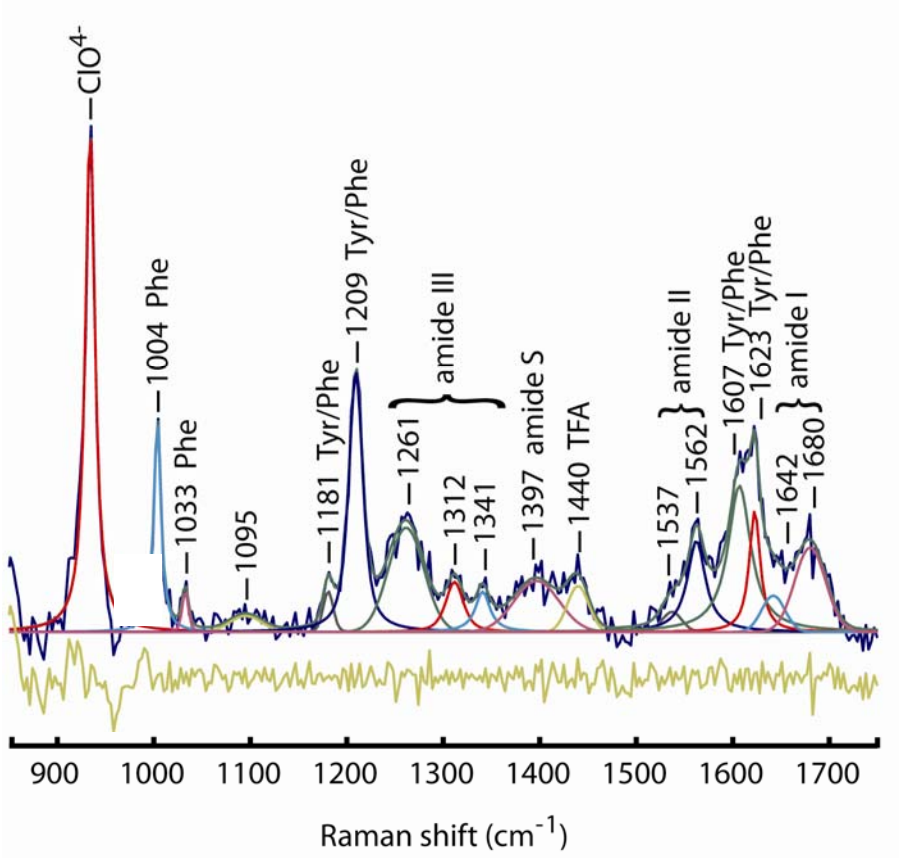

Figure 1.6 Pictured above is the initial UVRR spectrum of Aβ(1-16), at 195 nm excitation, with all the components in the deconvoluted fit. The bottom trace is the difference between the initial spectrum and calculated fit.

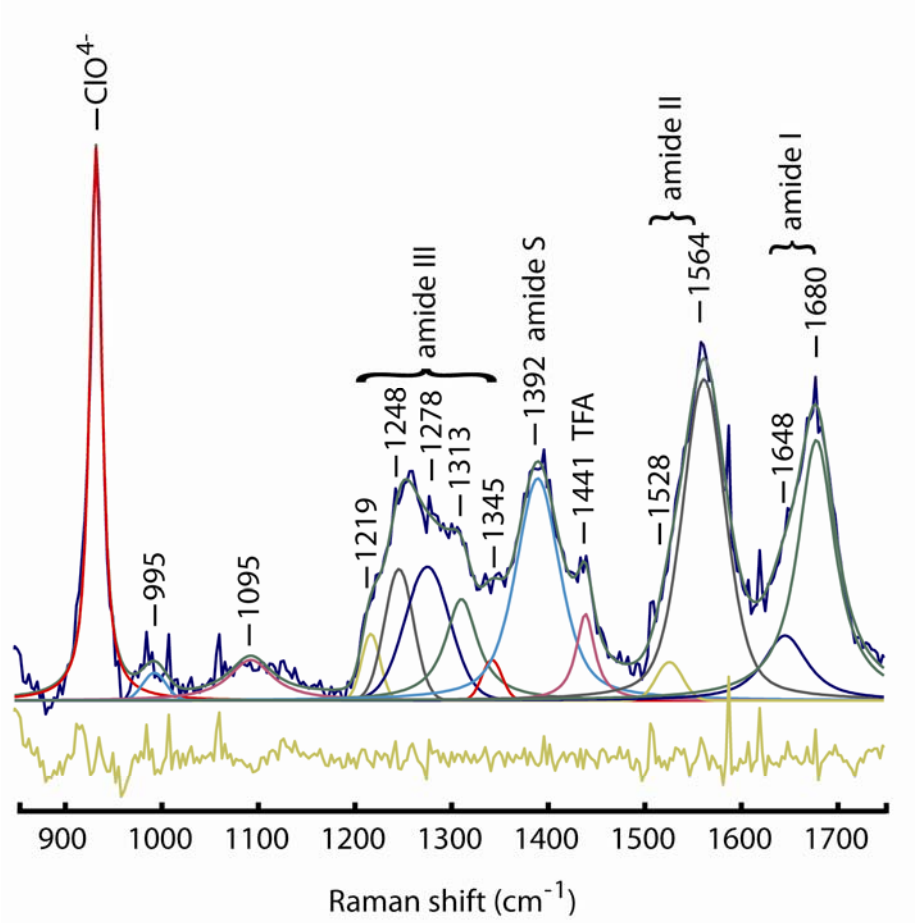

Figure 1.7 Pictured above is the initial UVRR spectrum of Aβ(25-40), at 195 nm excitation, with all the components in the deconvoluted fit. The bottom trace is the difference between the initial spectrum and calculated fit.

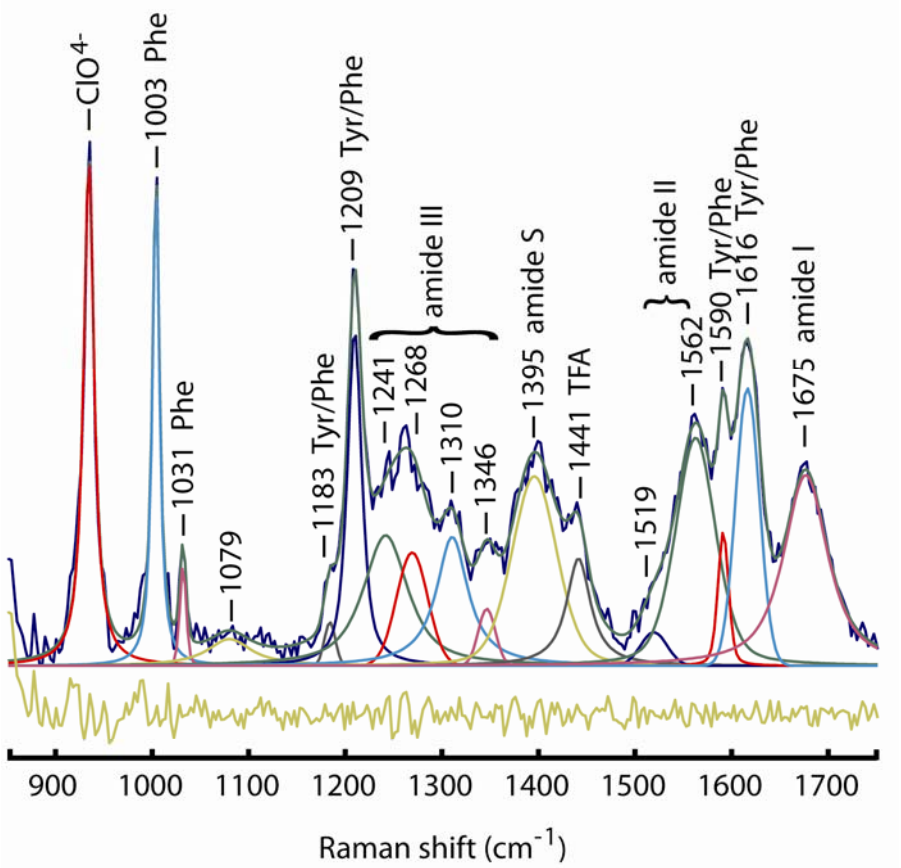

Figure 1.8 Pictured above is the initial UVRR spectrum of Aβ(1-40), at 195 nm excitation, with all the components in the deconvoluted fit. The bottom trace is the difference between the initial spectrum and calculated fit.

CHAPTER 2:

Elimination of Trifluoroacetic Acid from the HPLC Purification of the Beta-Amyloid Peptide

2.1 Introduction

Protein purification using reversed phase high performance liquid chromatography (RP-HPLC) requires the use of an ion-pairing agent, or counter-ion, to interact with the charged groups in the protein.[17] This increases the hydrophobic nature of the protein, meaning increased interaction with the hydrophobic stationary phase of the column, and achieving better separations.

Trifluoroacetic acid (TFA) is one of the most commonly used counter-ions in mobile phase solvents used in peptide and protein purification with RP-HPLC.[17] While TFA is effective in aiding separations, the residual TFA in the purified peptide can interfere with other spectroscopic studies, particularly UVRR and IR studies.[18, 19] TFA is not naturally present in the body, and the presence of TFA may modify the secondary structure of the Aβ peptide, which could potentially be problematic.[17] Previous research has shown that HCl can successfully replace the TFA in the RP-HPLC purification procedure.[18, 20] Both of these allow for reasonable separation of peaks in the chromatogram, but using HCl instead of TFA will remove the interfering peak of TFA which may show up in spectra of other techniques.[19, 20] The chloride ion from HCl is also found in the body and should therefore not unduly modify the secondary structure of the

Aβ peptide. For these reasons, HCl was chosen as an alternative to TFA in the further purification of crude Aβ(1-40) peptide.

In addition to modifying the counter-ion used, it was also necessary to determine the gradient method that provided the best peak separation. Initial studies conducted suggested that the Aβ(1-40) peptide eluted at approximately 45% acetonitrile (ACN) to 55% H_2O, so the gradient method developed focused around that range.

2.2 Theory

Reversed Phase – High Performance Liquid Chromatography. Normal phase HPLC involves a polar stationary phase and a non-polar mobile phase, whereas in reverse phase HPLC, there is a non-polar stationary phase and a polar mobile phase. Even though the normal phase was developed first and could correctly be referred to as just HPLC, the use of reverse phase HPLC has become much more common and as a result is often referred to simply as HPLC. For the remainder of the document, HPLC will mean reverse phase HPLC.

The non-polar stationary phase is made up of a porous silica bead that has long carbon chains attached to the surfaces of the bead.[21] The column used for this study was a C_{18} column, meaning the attached chains are 18 carbons in length. When a polar mobile phase solvent is used, non-polar molecules will interact more easily and be retained longer by these non-polar chains in the stationary phase. Using water as the initial mobile phase encourages interaction of the peptide with the non-polar chains of the stationary phase, while rapidly removing any polar impurities present in the sample. Gradually

increasing the concentration of the less polar acetonitrile into the mobile phase will then remove the peptide from the stationary phase.

The separation achieved is not only due to sorting polar from non-polar and all gradations in between, but it also sorts out the molecules partly based on surface area.[21] The more available non-polar surface area able to interact with the stationary phase, the longer it will be retained. This means that a long non-polar chain will be retained longer than a molecule that has the same number of carbons as the chain but is branched, not linear.

Mass Spectrometry. Mass spectrometry (MS) determines the mass of a molecule based on the separation of molecular ions by their mass-to-charge ratios. There are three components to every mass spectrometer: an ionization source, mass analyzer, and detector.[21] In this study, electrospray ionization (ESI) was used as the source of ions, followed by a triple-quadrupole mass analyzer, and detected using a photo-diode array detector.

With electrospray ionization, ions are produced when the liquid sample is forced through a needle via a very small capillary.[21] The capillary is heated, in this case to 250°C, and an electric charge (4.5 kV) is applied to the needle. What this does is create intact ions of the sample in an aerosol form. A neutral carrier gas like nitrogen is then used to gather up the ion cloud and move it into the mass analyzer.[21]

All mass analyzers will separate the ions formed on the basis of their mass-to-charge ratio (m/z). Ions with the same charge (z) will be equally affected by any change in the surrounding electromagnetic field, so any differences in the resulting trajectories will be solely a result of differences in mass.[21] The mass analyzer used for this study was

a triple-quadrupole spectrometer. More specifically, a quadrupole analyzer is made up of four charged metal rods where oppositely positioned rods have the same electrical charge. Radio frequencies are then applied across the metal rods as the ions are passed through. Only ions of a certain m/z will be able to pass through to the detector; all other ions will collide with the rods. Scanning through different radio frequencies allows for scanning of all the m/z states present.[7, 21]

The detector used in this study was a photodiode-array detector (PDA). A PDA is linear array of photodiodes, which are made up of a series of spaced *p*-type silicon bars set in an *n*-type silicon layer. The *p*-type regions contain positively-charged holes and the *n*-type regions have electrons. When the PDA is at rest, a depletion layer forms between the *p*-type and *n*-type regions at what is called the *pn* junction. This prevents the flow of electricity across the circuit. When photons hit the photodiode, the circuit is completed and the voltage produced is proportional to the intensity of the light hitting the photodiode.[21]

2.3 Experimental

2.3.1 Materials

Crude Aβ(1-40) was synthesized by Dr. Fabio Gallazzi, University of Missouri – Columbia. Commercially purified (>95%) Aβ(1-40) was purchased from Biopeptide (San Diego, CA). HPLC grade acetonitrile was purchased from Fisher (Pittsburgh, PA). DMSO (99%) and HPLC grade TFA were purchased from Sigma-Aldrich (St. Louis, MO).

2.3.2 Sample Preparation

HPLC Purification with TFA as counter-ion. Two mobile phase solvents were prepared using TFA as the counter-ion present. Ultrapure (18 MΩ) water with 0.1% TFA was prepared as Solvent A; ACN with 0.1% TFA was prepared as Solvent B. (By convention, the water/TFA solution is referred to as "Solvent A" because it is the aqueous phase, and the ACN/TFA solution is referred to as "Solvent B" because it is the organic phase.) Both solutions were degassed for at least 60 minutes, and the water/TFA solution was filtered through a Nalgene MF75 Series 500 mL filter unit (0.2 μm or 0.45 μm; SFCA membrane). It was not possible to filter the ACN/TFA solution through the filter because the ACN would destroy the membrane of the filter. The pH of each solvent was tested and found to be at or slightly above 2.0.

The crude Aβ(1-40) was dissolved in a 20% DMSO/Solvent A solution at a concentrations of approximately 3 mg/mL. The solution was centrifuged for 30 minutes at 4°C and 14,000 rcf. The supernatant was removed to an HPLC vial; the remainder was re-lyophilized for later use.

HPLC Purification with HCl as the counter-ion. Solvents were prepared with HCl as the counter-ion instead of TFA according to the same procedure outlined above. The crude Aβ(1-40) was also prepared in the same manner as the TFA counter-ion samples.

2.3.3 Measurements

For the purification procedure, a Beckman-Coulter HPLC (Fullerton, CA) equipped with a cooled auto-sampler tray (set to 7°C) was used with a Grace-Vydac 218tp54 (300Å, 5 µm, 4.6 mm ID x 250 mm) C_{18}-column (Deerfield, IL). The column was thoroughly flushed with Solvent A prior to purification.

The gradient used for purification of the crude Aβ(1-40) was: 0-40% Solvent B over 5 minutes; 40-80% Solvent B over 60 minutes; 80-100% Solvent B over 10 minutes. The flow rate was kept constant at 0.5 mL/min. Absorbance was measured at 280 nm versus time. Fractions were collected every 30 seconds using the fraction collector. All fractions coinciding with an eluent peak of interest were then lyophilized.

2.4 Results & Discussion

Commercial Aβ(1-40) was used initially with the gradient described above to determine a retention time, which was approximately 17 minutes, or about 47% Solvent B. (Figure 2.1) Based on these initial estimates, the crude Aβ was purified under the same method described above and several peaks were observed, one of which was at approximately 17 minutes. All peaks with an absorbance at 280 nm were collected and lyophilized, but only the sample from 17 minutes contained enough sample for further use. (Figure 2.2) The presence of Aβ(1-40) was verified using MS.

Substituting HCl for TFA with the same gradient method outlined above, the purified Aβ(1-40) eluted at about 19 minutes instead of 17 minutes, with about the same yield, as verified with MS. The corresponding solvent composition was ~49% Solvent B.

The peaks also appear narrower and are slightly more resolved from one another as compared to the TFA purification. (Figure 2.3)

It was also possible to continue the purification of the Aβ(1-40) by repeating the procedure outlined above using Aβ(1-40) that has already been purified once instead of using the crude Aβ(1-40). One difficulty with this substitution is that much less than 3 mg of purified Aβ was available for further purification. The resulting chromatograms were much cleaner, and the peak of interest was much more prominent. (Figure 2.4) The percent yield is likely about the same, but because so little Aβ was available to use initially (~0.2 mg), there was not enough peptide remaining after lyophilization for further use.

The two peaks with retention times near 17 minutes are not well-resolved and are visible in the chromatograms for both Solvent B compositions. Using the current gradient and collection method, those two peaks are collected together in the same fraction and essentially re-mixed. This is likely the source of the contamination seen in the MS results, though it is unclear what the contaminant may be.

2.5 Conclusion

This study shows that using HCl as the counter-ion in the HPLC mobile phase solvents is at least as effective in aiding peptide separation and purification as using the more traditional counter-ion, TFA. The benefit to using HCl instead is that it removes the need for and presence of TFA in the sample, which has been shown to interfere with other spectroscopic methods like UVRR and IR-Raman, and may adversely modify the secondary structure of the Aβ peptide.

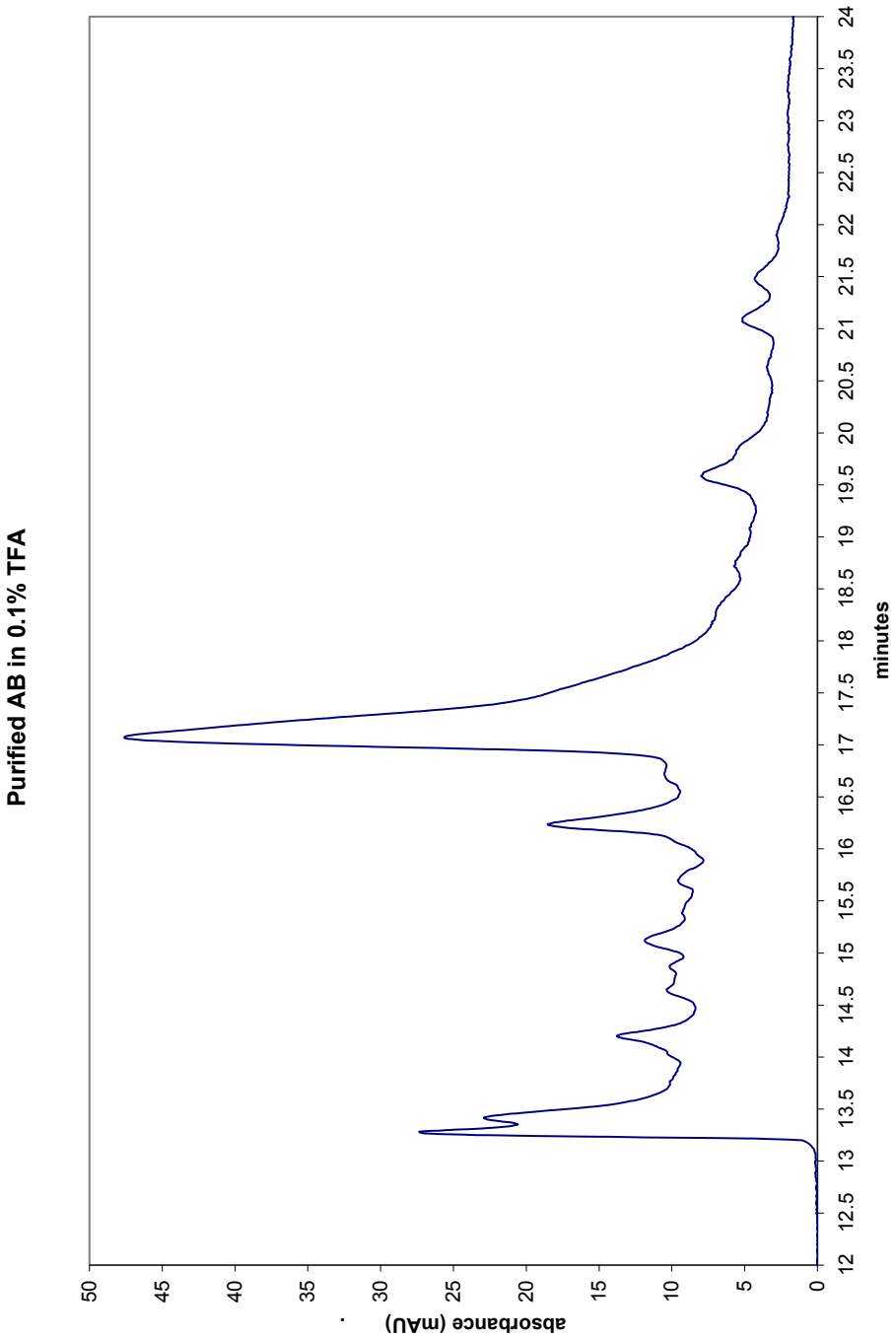

Figure 2.1 HPLC chromatogram of commercially purified Aβ(1-40) in 0.1% TFA.

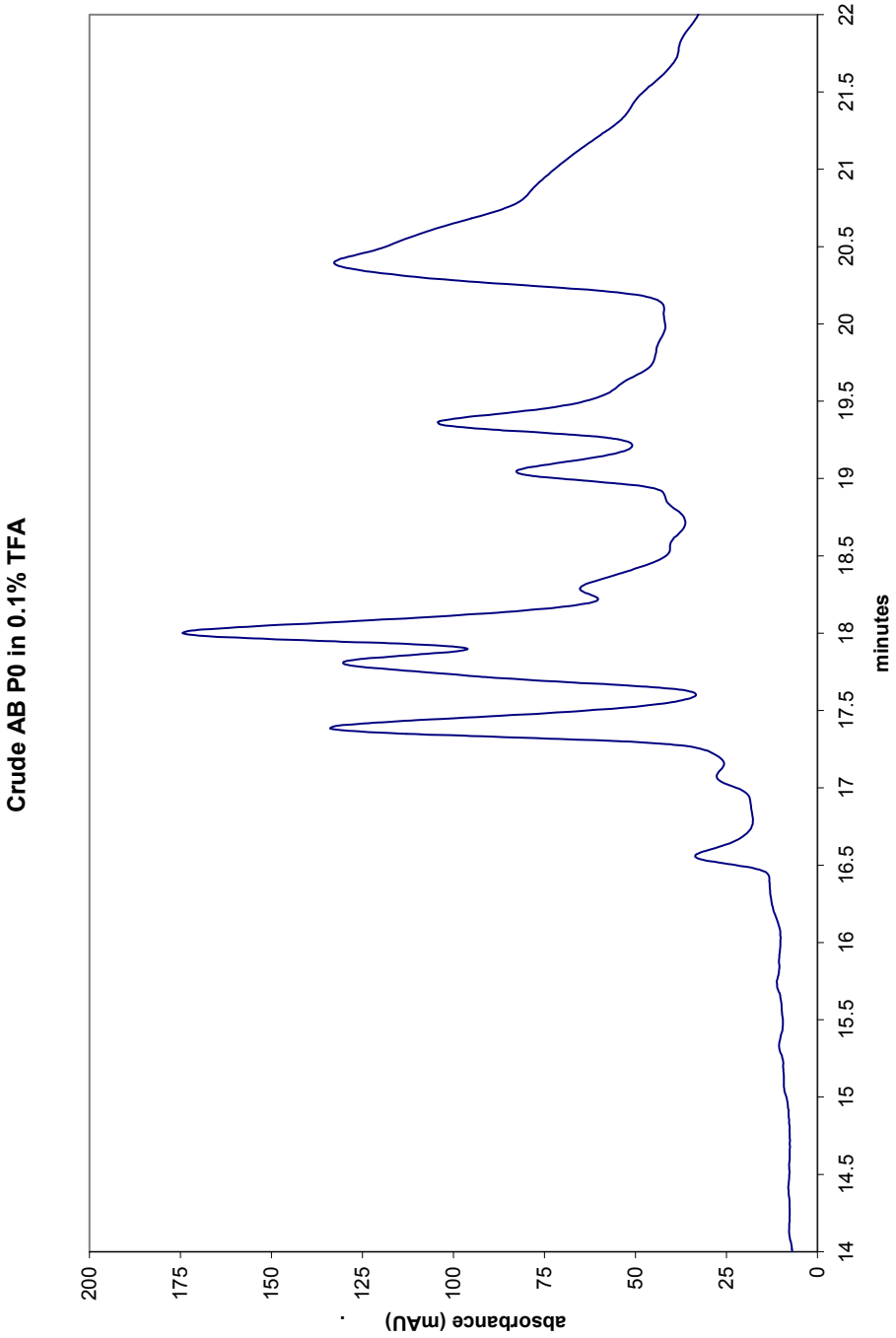

Figure 2.2 HPLC chromatogram of first-run purification of Aβ(1-40) in 0.1% TFA.

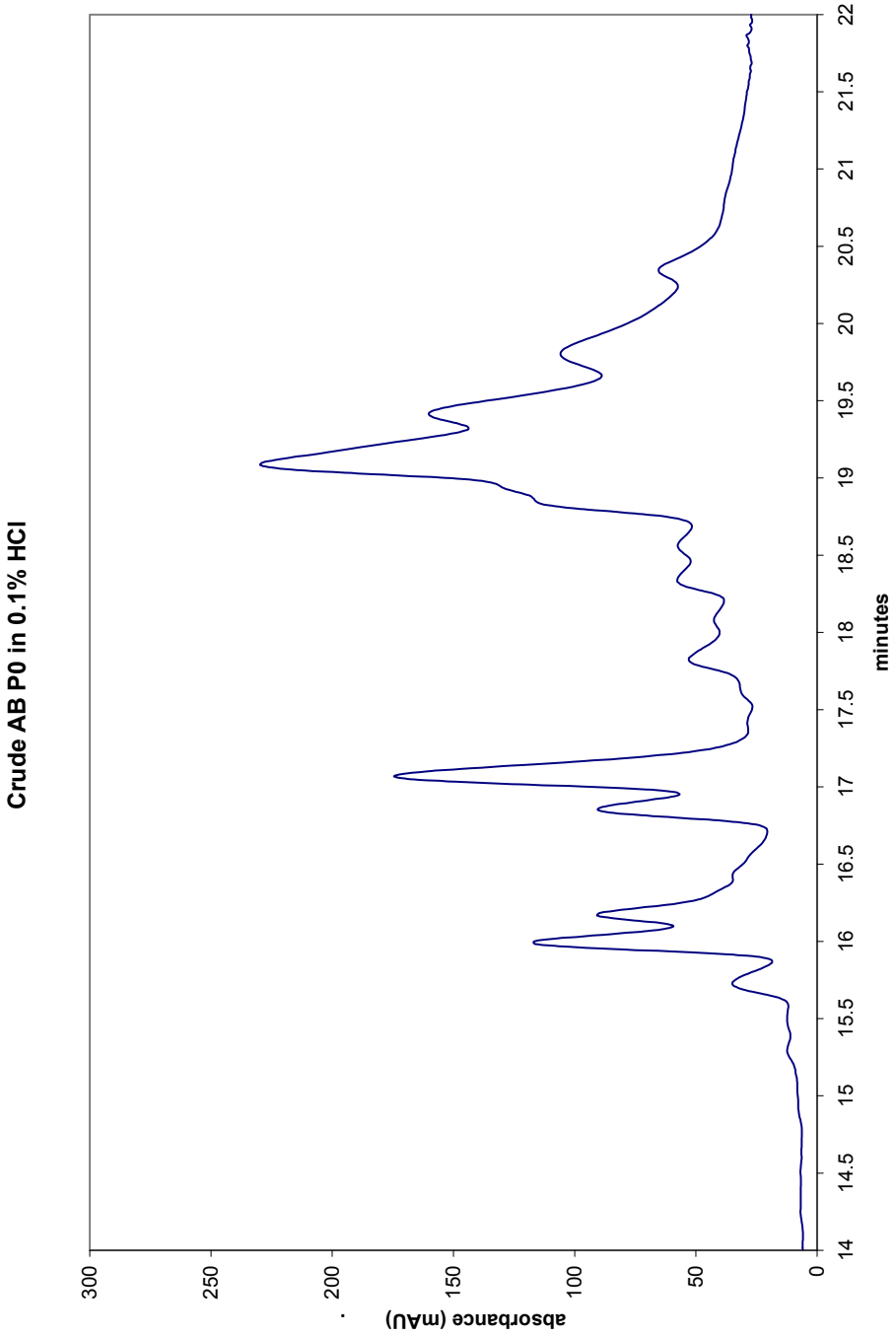

Figure 2.3 HPLC chromatogram of first-run purification of Aβ(1-40) in 0.1% HCl.

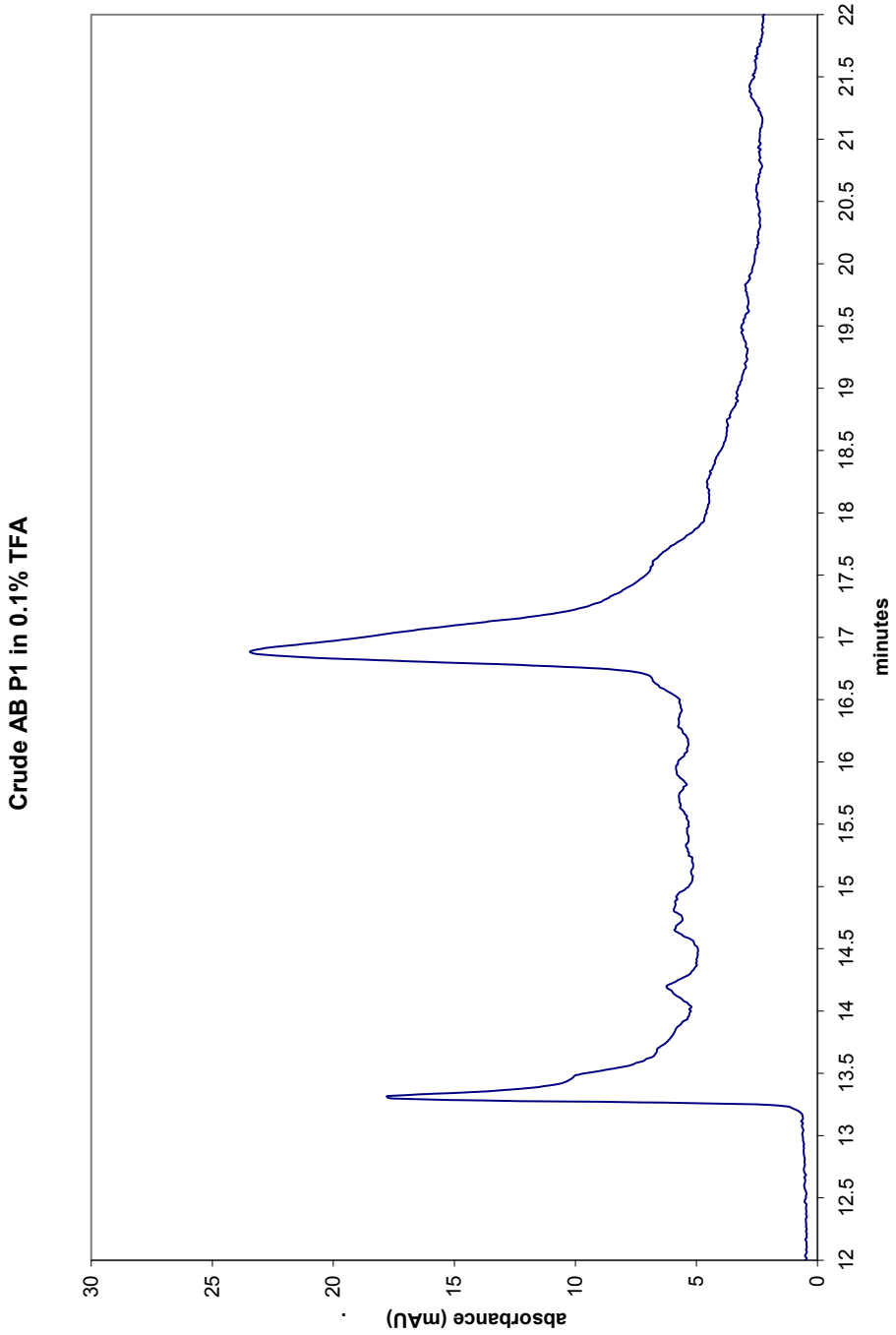

Figure 2.4 HPLC chromatogram of second-run purification of Aβ(1-40) in 0.1% TFA.

CHAPTER 3:

Quantifying Extended (Disordered) Peptides: Evaluation of the Performance of Three Different Methods

3.1 Introduction

There are several available methods used for determining protein concentration, but each has certain strengths and limitations. Some of the more common options include protein assays, estimation using absorbance and molar extinction coefficients, and amino acid analysis.

Protein assays, such as the Bradford or Lowry assays, are quite common, but there are several limitations.[22] First, it is necessary to choose a protein standard that has a similar composition to the protein to be assayed. In the Lowry assay, it is the number of tyrosine residues that is detected, and that number is variable among proteins.[22] The Bradford assay uses a dye that binds to the basic residues of the protein, so it is important to find a standard protein that has a similar number of basic residues. Second, the presence of common buffer components like tris and EDTA can interfere with the results of the assay.[22] Third, there is additional error introduced because of required incubation for the assay.[22] Variations in the length of incubation will create irreproducible results. Finally, the effective concentration ranges for these assays are limited. The Lowry assay detects between 2 and 100 μg/mL of protein; the Bradford assay detects between 0.2 and 20 μg/mL of protein.[22]

Amino acid analysis is arguably the best method for determining protein concentrations, but is not readily available for most laboratories and may be prohibitively expensive for routine analysis.[22]

One other commonly accepted method for estimating the concentration of peptides involves taking the absorbance of the peptide and using the molar extinction coefficient.[21] Calculating the true molar extinction coefficient for a peptide can be problematic, particularly if the peptide happens to be costly. To get around this, the absorbance and molar extinction coefficients of aromatic amino acids are often used instead. One example is that of tyrosine (ε_{280}=1280 $M^{-1}cm^{-1}$) for estimating the concentration of the Aβ peptide. Because this method focuses on an absorbance response collected at a single point of the spectrum, it can be referred to as a univariate method, or zero-order calibration method.[23, 24] Univariate linear regression is generally used for developing calibration curves because the concentration value is linked directly to only a single point response.[24]

A multivariate linear regression approach, or first-order calibration, will incorporate more of the absorbance spectrum in the concentration estimates than a single point as in univariate analysis.[23, 24] This should lead to more accurate concentration predictions because it is equivalent to making several different univariate calculations at once and combining the results into a more robust prediction.[24] Also, using multivariate analysis should reduce the overall error because the background noise and contribution from other components like buffer can be modeled and removed.[24] The particular multivariate method used in this study was principal component regression (PCR).

3.2 Theory

Absorbance. Absorbance is a measurement of the energy required to transition a molecule from the ground state (S_0) to an excited state (S_n).[21] The shorter the wavelength of light, the higher the energy and better capability for promoting the molecule to higher excited states. Typically the wavelengths used will only be enough to promote the molecule to either the S_1 or S_2 excited states.[21] Absorption peaks are generally broad because the energy absorbed can correspond to any of a number of vibrational levels within the same excited state.[21] Absorbance (A) can be directly related to concentration using the Beer-Lambert Law, where ε is the molar extinction coefficient (M^{-1} cm^{-1}), b is the cell path length (cm), and c is the sample concentration (mol L^{-1}).

$$A = \varepsilon * b * c \qquad \text{(Eq. 3.1)}$$

Molar extinction coefficients of the amino acid residues tyrosine (ε_{280}=1280 M^{-1} cm^{-1}) and tryptophan (ε_{278}=5579 M^{-1} cm^{-1}) are commonly used to estimate the concentration of peptides in solution. Even though calculating the actual molar extinction coefficient of the individual peptide at known concentrations and then using that value for subsequent concentration determinations would be more accurate, that may not always be possible, for instance, in cases where the peptide being studied is expensive or perhaps hard to dissolve. In such instances, estimating the concentration using tyrosine or tryptophan may be sufficient.

Principal Component Regression. Principal component regression (PCR) is a multivariate calibration analysis based on the principal components present in the data.[25, 26] A principal component defines variability in the data, ultimately reducing the dimensionality of the data while retaining the most important information about that

data.[25, 26] For instance, the first principal component describes the maximum variation in the data, then the second principal component would be arranged orthogonal to the first and describe the next greatest amount of variation, and so on.[25, 26]

PCR is better than other multivariate methods at analyzing data where the variables are significantly correlated, because the number of principal components required to describe the data will be significantly reduced, and those principal components will not be correlated to one another, thus allowing for better concentration predictions.[25, 26]

To explain how PCR works, it is first necessary to explain principal component analysis (PCA) and singular value decomposition (SVD). PCA is the process where the original data matrix, **X**, is broken down into two matrices, **T** and **L**.[25, 26] The **T** matrix is called the scores matrix, containing the original number of rows present in **X** and as many columns as there are principal components (k). The **L** matrix, or loadings matrix, contains as many rows as there are principal components and the number of columns present in the original matrix, **X**.[25, 26] The result from multiplying **T** and **L** is the original data matrix **X**.

$$X_{n.,p} = T_{n,k} L_{k,p} \qquad \text{(Eq. 3.2)}$$

SVD is similar to PCA in that it creates a scores matrix (**U**) and loadings matrix (**V**).[25, 26] However, instead of directly relating the two by the number of components as before, another matrix is introduced between the scores and loadings matrices. This matrix (**S**) contains the calculated square-roots of the eigenvalues in decreasing magnitude along the diagonal from top-left to bottom-right. All other values in the **S** matrix are zero.[25, 26] The dimensions of the **S** matrix are equivalent to the number of

principle components. The values in the **S** matrix act to lend appropriate weight to the resulting values according to the principal components. The first principal component will have the largest corresponding value in the **S** matrix, and so on.[25, 26]

$$X_{n,p} = U_{n,k} S_{k,k} V'_{k,p} \qquad \text{(Eq. 3.3)}$$

The PCR process actually begins by performing an SVD analysis of the response data, in this case the absorption data matrix. The values for the matrices formed by SVD are then used to calculate the regression coefficient, **b**, according to the following equation:

$$b_{p,1} = V_{p,k} S^{-1}_{k,k} U'_{k,n}\, y_{n,1} \qquad \text{(Eq. 3.4)}$$

where the **y** vector contains the dependent concentration variables for the response matrix, **X**.[25, 26] The calculated regression coefficient can then be multiplied by the unknown response data to determine a concentration estimate.[25, 26]

Amino Acid Analysis. Amino acid analysis is a highly accurate method for determining protein concentration. The general procedure begins by breaking down the protein into the individual amino acids through acid hydrolysis. The freed amino acids are then separated using HPLC. The collected values are then compared to known amino acid standards, thereby determining a concentration for each individual residue present in the sample. Those concentrations can then be summed up and an overall protein concentration can be determined.

3.3 Experimental

3.3.1 Materials

The Aβ(1-40) had greater than 95% purity and was purchased from Biopeptide (San Diego, CA). Angiotensin II and glucagon (1-29) were purchased from Global Peptide (Fort Collins, CO) at 96% purity. Endomorphin I was purchased from Sigma (99.8% purity). The phenylalanine, tyrosine, and tryptophan were obtained from Fluka (99% purity). Phosphate buffer components and HPLC grade ammonium hydroxide were purchased from Fisher (Pittsburgh, PA).

3.3.2 Sample Preparation

Initial solutions were prepared by dissolving 0.1 mg of phenylalanine, tyrosine, or tryptophan into 1.0 mL of 10mM phosphate buffer. The resulting solutions were then used to make 200μM stock solutions of each. Those stock solutions were then used to prepare a series of 16 standards containing both mixed and pure samples of phenylalanine, tyrosine, and tryptophan.

The Aβ(1-40) solutions were prepared by dissolving 0.5 mg of Aβ peptide into 50 μL of 0.1 M NH_4OH. All solutions were kept at 5°C. The Aβ solutions were then slowly diluted to 500 μL with ultra-pure water. The resulting concentration of Aß was approximately 230 μM. Concentrated phosphate buffer was then added to the solution, resulting in a concentration of 10 mM phosphate buffer. The solutions were then pH adjusted to 7.4.

Solutions of angiotensin II were prepared by dissolving 1.0 mg into 1.0 mL of 10 mM phosphate buffer. The maximum theoretical concentration based on mass of peptide

used was 965 μM. Solutions of the peptides endomorphin I and glucagon(1-29) were prepared by dissolving 0.5 mg of each in 1.0 mL of 10mM phosphate buffer and sonicating for 2 minutes. The resulting theoretical maximum mass-based concentrations were approximately 450 μM and 144 μM, respectively.

3.3.3 Measurements

Absorbance measurements from 200 to 600 nm were taken using a 1 cm path-length quartz cuvette from Hellma (Plainview, NY) in an HP 8453 UV-Vis Spectrophotometer (Agilent, Santa Clara, CA).

3.3.4 Data Analysis

All calculations were performed using MatLab (MathWorks, Natick, MA). For each of the absorbance spectra collected, any contribution from the buffer was removed. Then the baselines were corrected by determining a best-fit linear line to a portion of the spectrum that should not have any contribution from absorbance, namely 320 -400 nm, and then subtracting that best fit line from the entire spectrum. For the univariate calculations, only the wavelength 280 nm was used. For multivariate analyses, wavelengths from 240 to 300 nm were used.

In this study, a set of 16 standards was used to estimate concentration of four samples: Aβ(1-40); angiotensin II; endomorphin I; and glucagon(1-29). The standards were composed of phenylalanine, tyrosine, and tryptophan in varied concentrations. The standard concentrations used are listed in Table 3.1. Regression parameters were then calculated based on the standards according to the PCR method described above.

Multiplying the values for the unknown samples by the calculated regression vector yielded the concentration estimates listed in Table 3.2. The PCR program developed for this study is included in the appendix.

Table 3.1 Amino acid concentrations in standards used in PCR

	Concentration (μM)		
Sample	Phe	Tyr	Trp
1	100	0	0
2	75	25	0
3	50	50	0
4	25	75	0
5	75	0	25
6	50	0	50
7	25	0	75
8	0	0	100
9	0	25	75
10	0	50	50
11	0	75	25
12	0	100	0
13	50	50	50
14	75	25	25
15	25	75	25
16	25	25	75

Table 3.2 Theoretical and calculated concentration estimates for four peptides

	Concentration (μM)					
	Max. Theoretical°	AAA	Univariate		Multivariate	
			Tyr	Trp	Tyr	Trp
Aβ(1-40)	219	145	230 ± 70^	-*	130 ± 40^	-*
angiotensin II	917	755	420 ± 20^	-*	590 ± 20^	-*
glucagon(1-29)	138	84	-**	100 ± 40^	-**	120 ± 50^
endomorphin I	817	494	-**	450^^	-**	500^^

(°): Max. theoretical values are calculated from the measured mass and weighted against the purity of the sample

(^): For all standard deviations, n=3.

(^^): Error was not calculated for this peptide

(*): No Trp residues in peptide

(**): Greater Trp ε prevents reasonable estimation of Tyr concentration

3.4 Results & Discussion

The absorption wavelengths isolated for calculations used in this study were 240 to 300 nm. Even though the region from 200 to 300 nm potentially held more information, more accurate results were obtained by focusing on just the region from 240 to 300 nm. All amino acids will absorb in the deep UV, particularly from 200 to 220 nm, due to the amino acid backbone strongly absorbing in that wavelength region. Only the aromatic amino acids will also have characteristic absorbance patterns between 240 and 300 nm. (Figure 3.1) The reason for this is due to the bonds in the rings comprising the functional groups of the aromatic amino acids absorbing in this region.

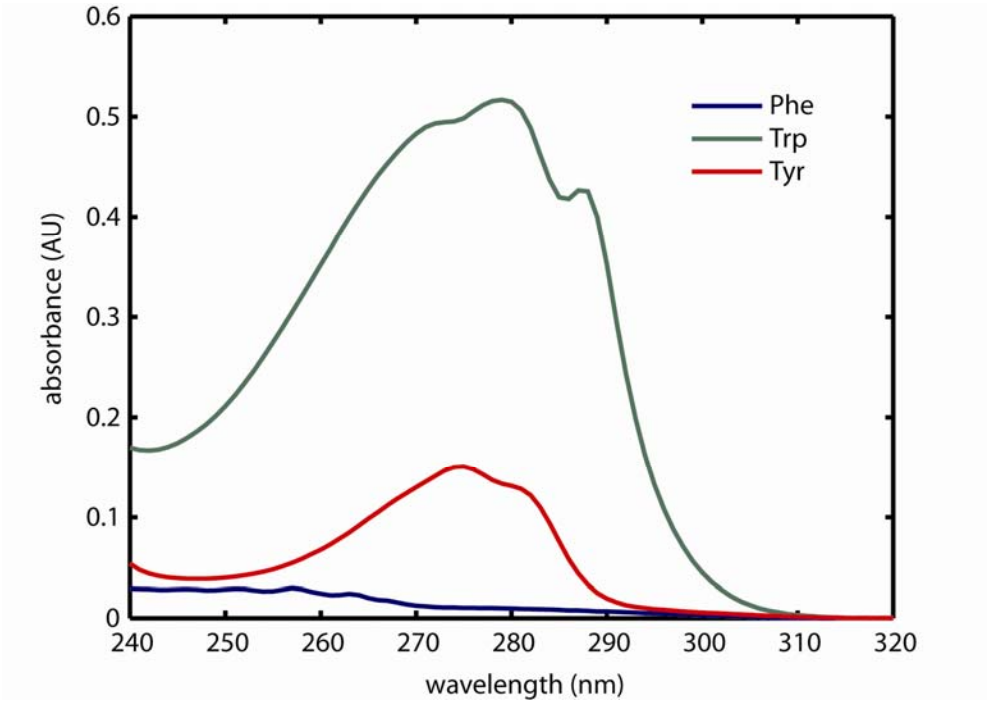

Figure 3.1 A comparison of the relative absorbance intensities of 100 μM phenylalanine, tyrosine, and tryptophan.

As can be seen in Figure 3.1, the absorbance of tryptophan near 280 nm is much more pronounced than that of tyrosine, and the tryptophan absorbance dwarfs that of phenylalanine. The drastic differences in relative intensity of the absorbance of the three amino acids at the same concentrations proved problematic. The PCR technique is only effective at determining the phenylalanine concentration when neither tryptophan or tyrosine is present. It is not possible to resolve the absorbance of phenylalanine from the other two amino acids when they are present. The molar absorptivity of phenylalanine is simply too low. Likewise, when tryptophan and tyrosine are present in a peptide, the absorbance of the tryptophan will overlap and be much greater than that of the tyrosine, so that using the molar extinction coefficient of tyrosine to make concentration estimates without modifying it to take tryptophan into consideration could lead to wildly incorrect concentration estimates. Even so, the contribution from tyrosine is not insignificant at 280 nm. Initially, PCR seemed as though it would be a good alternative for resolving the two components because it would use more of the absorbance spectrum. Interestingly, there is little difference in the values calculated using the univariate method versus the multivariate method when tryptophan is present in the peptide.

The Aβ(1-40) peptide was used initially to determine the applicability of the PCR method to figuring the relative concentration of phenylalanine and tyrosine in the peptide. While determining the concentration of phenylalanine did not work as expected, due to reasons described above, the determination of tyrosine was quite effective. The PCR method returned an estimate of 130 μM tyrosine, which corresponds to the same concentration for Aß because there is just one tyrosine present in the peptide. Using the univariate method of calculating the concentration based on absorbance at 280 nm and a

molar extinction coefficient for tyrosine of 1280 M^{-1} cm^{-1}, the resulting estimate was significantly different at 230 μM tyrosine/beta-amyloid. Amino acid analysis (AAA) returned a concentration of 145 μM tyrosine/beta-amyloid, but the theoretical maximum calculated was closer to 220 μM. This helps to illustrate the extreme difficulty in obtaining accurate measurements of concentration.

Other peptides were used to determine the applicability of the PCR method for tyrosine and tryptophan concentration determinations. The concentrations of angiotensin II, endomorphin I, and glucagon(1-29) were estimated based on absorbance, both by molar extinction coefficients and by PCR. Theoretical maximum concentrations were calculated using the measured mass (assuming no error in the measurement) and weighting the value against the reported purity of the sample. [Molecular weights and amino acid sequence data for all four peptides is included in the appendix.] Actual concentrations were determined using AAA.

Using PCR on the absorbance data for angiotensin II resulted in a value of 590 μM. There is one tyrosine and no tryptophan present in the peptide. The molar extinction coefficient of tyrosine at 280 nm yields a value of 420 μM tyrosine/angiotensin II. Again the values are significantly different. AAA yielded a result of 755 μM, and the theoretical maximum was 917 μM. Glucagon(1-29) contains two tyrosine residues and one tryptophan residue. Absorbance at 280 nm gave a total concentration estimate of 100 μM, while PCR returned a value of 120 μM Trp. AAA yielded a concentration of 84 μM, and the theoretical maximum was 138 μM. Endomorphin I contains one tyrosine and one tryptophan residue. Univariate absorbance returned a concentration of 450 μM, and PCR

predicted 500 μM. AAA returned a value of 494 μM, and the theoretical maximum was 817 μM.

3.5 Conclusion

The PCR method seems to be about as effective at predicting concentration as the standard method of using molar extinction coefficients, at least when tryptophan is the focus. (Table 3.2) There was very little difference between the predicted concentration values using the univariate and multivariate methods for the tryptophan-containing peptides. Both sets of concentration values for the tryptophan-containing peptides were slightly higher than the concentration value obtained with AAA. This is likely due to the fact that tyrosine was also present in those peptides. Even though the tyrosine could not be resolved for concentration estimation, its presence is significant enough to affect the prediction of tryptophan concentration. The multivariate method was slightly better at predicting the concentration of peptides when no tryptophan was present when compared to the values obtained with the univariate method. These mixed results regarding the univariate and multivariate methods indicate that PCR does not provide any distinct advantage over using the more traditional univariate method of calculating concentration based on molar extinction coefficients.

SUMMARY

This project focused on looking at the native structure of the Aβ peptide and a few of the difficulties encountered when trying to perform structural studies. The first part of the study compared the CD and UVRR results of the three fragments of the Aβ peptide. Both CD and UVRR suggest that the hydrophilic Aβ(1-16) fragment is predominantly PPII structure, and that the hydrophobic Aβ(25-40) fragment is more disordered and β-strand conformation. The Aβ(1-40) fragment displayed aspects of both shorter fragments, as well as possible β-sheet structure.

The second and third parts of this study looked at problems associated with determining the secondary structure of the Aβ peptide. The commonly used counter-ion in HPLC purifications, TFA, has an interfering band that shows up in UVRR and IR spectra. It has also been shown to alter the secondary structure of other peptides, and may do the same to the Aβ peptide. To address this, HCl was used as an alternative counter-ion for Aβ peptide purification. Similar results were obtained with both counter-ions.

Another problem associated with studying the Aβ peptide is being able to accurately estimate the concentration. The third part of the study attempted to find a better way to estimate the concentration of peptide in solution. Every method currently used has both benefits and limitations. This part primarily compared the effectiveness of the absorbance-based univariate and multivariate methods of concentration estimation against the concentrations obtained with AAA. When tryptophan is present in the peptide, there was very little difference between the estimates obtained with univariate versus multivariate methods. When tyrosine is used for the estimations and tryptophan is not

present, the multivariate approach produced slightly more accurate estimations than the univariate methods. Even so, there was no distinct advantage to using a multivariate approach over a univariate approach.

BIBLIOGRAPHY

1. Atwood, C. S.; Martins, R. N.; Smith, M. A.; Perry, G., Senile plaque composition and posttranslational modification of amyloid-[beta] peptide and associated proteins. *Peptides* **2002,** 23, (7), 1343-1350.

2. De Felice, F. G.; Vieira, M. N. N.; Saraiva, L. M.; Figueroa-Villar, J. D.; Garcia-Abreu, J.; Liu, R. O. Y.; Chang, L. E. I.; Klein, W. L.; Ferreira, S. T., Targeting the neurotoxic species in Alzheimer's disease: inhibitors of A-beta oligomerization. *FASEB J.* **2004,** 18, (12), 1366-1372.

3. Walsh, D. M.; Selkoe, D. J., Aß Oligomers - a decade of discovery. *Journal of Neurochemistry* **2007,** 101, (5), 1172-1184.

4. Zheng, H.; Koo, E., The amyloid precursor protein: beyond amyloid. *Molecular Neurodegeneration* **2006,** 1, (1), 5.

5. Danielsson, J.; Jarvet, J.; Damberg, P.; Graslund, A., The Alzheimer beta-peptide shows temperature-dependent transitions between left-handed 3(1)-helix, beta-strand and random coil secondary structures. *Febs Journal* **2005,** 272, (15), 3938-3949.

6. Tiffany, M. L.; Krimm, S., Circular Dichroism of the "Random" Polypeptide Chain. *Biopolymers* **1969,** 8, 347-359.

7. Hammes, G. G., *Spectroscopy for the Biological Sciences*. John Wiley & Sons, Inc.: Hoboken, NJ, 2005.

8. Greenfield, N.; Fasman, G., Computed Circular Dichroism Spectra for Evaluation of Protein Conformation. *Biochemistry* **1969,** 8, (10), 4108-4116.

9. Smith, E.; Dent, G., *Modern Raman Spectroscopy*. John Wiley & Sons, Inc.: Hoboken, NJ, 2005.

10. Asher, S. A., UV resonance Raman studies of molecular structure and dynamics: applications in physical and biophysical chemistry. *Annual Review of Physical Chemistry* **1988,** 39, 537.

11. Chi, Z.; Chen, X. G.; Holtz, J. S. W.; Asher, S. A., UV Resonance Raman-Selective Amide Vibrational Enhancement: Quantitative Methodology for Determining Protein Secondary Structure. *Biochemistry* **1998,** 37, (9), 2854-2864.

12. JiJi, R. D.; Balakrishnan, G.; Hu, Y.; Spiro, T. G., Intermediacy of Poly(L-proline) II and β-Strand Conformations in Poly(L-lysine) β-Sheet Formation Probed by Temperature-Jump/UV Resonance Raman Spectroscopy. *Biochemistry* **2006,** 45, (1), 34-41.

13. Wang, Y.; Purrello, R.; Jordan, T.; Spiro, T. G., UVRR Spectroscopy of the Peptide Bond. I. Amide S, a Nonhelical Structure Marker, Is a C{alpha}-H Bending Mode. *J. Am. Chem. Soc.* **1991,** 113, 6359-6368.

14. Sane, S. U.; Cramer, S. M.; Przybycien, T. M., A Holistic Approach to Protein Secondary Structure Characterization Using Amide I Band Raman Spectroscopy. *Analytical Biochemistry* **1999,** 269, 255-272.

15. Austin, J. C.; Jordan, T.; Spiro, T. G., Ultraviolet Resonance Raman Studies of Proteins and Related Model Compounds. In *Biomolecular Spectroscopy, Part A*, Clark, R. J. H., Ed. John Wiley & Sons, Inc.: Hoboken, NJ, 1993; pp 55-127.

16. Asher, S. A.; Mikhonin, A. V.; Bykov, S., UV Raman Demonstrates that [alpha]-Helical Polyalanine Peptides Melt to Polyproline II Conformations. *JACS* **2004,** 126, 8433-8440.

17. García, M. C., The effect of the mobile phase additives on sensitivity in the analysis of peptides and proteins by high-performance liquid chromatography-electrospray mass spectrometry. *Journal of Chromatography B* **2005,** 825, (2), 111-123.

18. Gaussier, H.; Morency, H.; Lavoie, M. C.; Subirade, M., Replacement of Trifluoroacetic Acid with HCl in the Hydrophobic Purification Steps of Pediocin PA-1: a Structural Effect. *Appl. Environ. Microbiol.* **2002,** 68, (10), 4803-4808.

19. Stéphane Roux, E. Z. B. R. M. P. J.-C. C. N. F., Elimination and exchange of trifluoroacetate counter-ion from cationic peptides: a critical evaluation of different approaches. *Journal of Peptide Science* **2008,** 14, (3), 354-359.

20. Nilsson, M. R.; Nguyen, L. L.; Raleigh, D. P., Synthesis and Purification of Amyloidogenic Peptides. *Analytical Biochemistry* **2001,** 288, (1), 76-82.

21. Skoog, D. A.; Holler, F. J.; Crouch, S. R., *Principles of Instrumental Analysis*. 6th ed.; Thomson Higher Education: Belmont, CA, 2007.

22. Knight, M.; Chambers, P., Problems associated with determining protein concentration. *Molecular Biotechnology* **2003,** 23, (1), 19-28.

23. Booksh, K. S.; Kowalski, B. R., Theory of analytical chemistry. *Anal. Chem.* **1994,** 66, (15), 782-791.

24. Otto, M., *Chemometrics: Statistics and Computer Application in Analytical Chemistry*. Wiley-VCH: Weinheim, Germany, 1999.

25. Miller, J. N.; Miller, J. C., *Statistics and Chemometrics for Analytical Chemistry*. 4th ed.; Pearson Education Limited: Essex, England, 2000.

26. Egan, W. J., Measurement of carboxyhemoglobin in forensic blood samples using UV-visible spectrometry and improved principal component regression. *Applied Spectroscopy* **1999,** 53, (2), 218.

APPENDIX

A.1 UVRR Band Assignment Parameters

		ClO^(4-)	Phe	Phe	PO^(4-)	Tyr/Phe	Tyr/Phe
AB(1-40)	position	933.51	1003.03	1031.03	1079.10	1183.10	1208.72
	height	298.53	291.34	58.47	15.64	25.47	196.29
	FWHM	12.71	8.40	7.89	55.00	13.39	17.77
	%Lorenzian	1.00	1.00	0.28	1.00	0.00	0.73
AB(1-16)	position	933.91	1003.71	1032.52	1095.20	1180.73	1209.39
	height	223.68	94.36	18.05	7.08	17.88	115.18
	FWHM	11.80	8.55	7.60	38.90	12.23	17.29
	%Lorenzian	1.00	1.00	0.39	0.00	0.21	0.71
AB(25-40)	position	934.39			1094.72		
	height	484.20			35.65		
	FWHM	14.95			55.00		
	%Lorenzian	0.88			1.00		

		amide III					amide S
AB(1-40)	position		1240.86	1268.30	1309.82	1345.64	1394.86
	height		76.04	66.01	75.14	33.22	110.51
	FWHM		55.00	38.00	39.54	20.92	55.00
	%Lorenzian		0.78	0.00	1.00	0.00	0.25
AB(1-16)	position			1261.47	1311.68	1340.79	1396.74
	height			45.80	22.02	17.75	22.42
	FWHM			43.46	21.80	18.34	55.00
	%Lorenzian			0.00	0.62	1.00	0.00
AB(25-40)	position	1219.10	1248.24	1277.65	1312.91	1344.52	1392.02
	height	58.52	114.70	116.85	89.13	35.77	194.22
	FWHM	22.59	35.44	55.00	40.46	24.24	54.02
	%Lorenzian	0.00	0.00	0.08	1.00	0.00	0.57

(continued on next page)

		TFA	amide II		Tyr/Phe	Tyr/Phe	amide I	
AB(1-40)	position	1440.58	1518.53	1561.84	1590.46	1615.61		1675.85
	height	62.64	19.59	132.94	78.02	161.54		111.22
	FWHM	30.01	32.40	49.10	13.02	29.04		54.17
	%Lorenzian	1.00	0.00	0.35	0.34	0.00		0.78
AB(1-16)	position	1439.76	1537.06	1562.44	1607.05	1622.91	1642.12	1680.31
	height	20.17	8.85	39.99	64.17	53.40	15.95	37.04
	FWHM	26.08	24.20	22.68	28.50	13.59	28.50	37.73
	%Lorenzian	0.00	0.00	1.00	1.00	1.00	0.00	0.00
AB(25-40)	position	1441.33	1528.26	1563.97			1648.11	1680.48
	height	76.00	33.80	282.07			57.00	227.94
	FWHM	23.15	31.65	52.46			55.00	46.48
	%Lorenzian	1.00	0.00	0.42			0.86	0.96

A.2 MS Raw Data

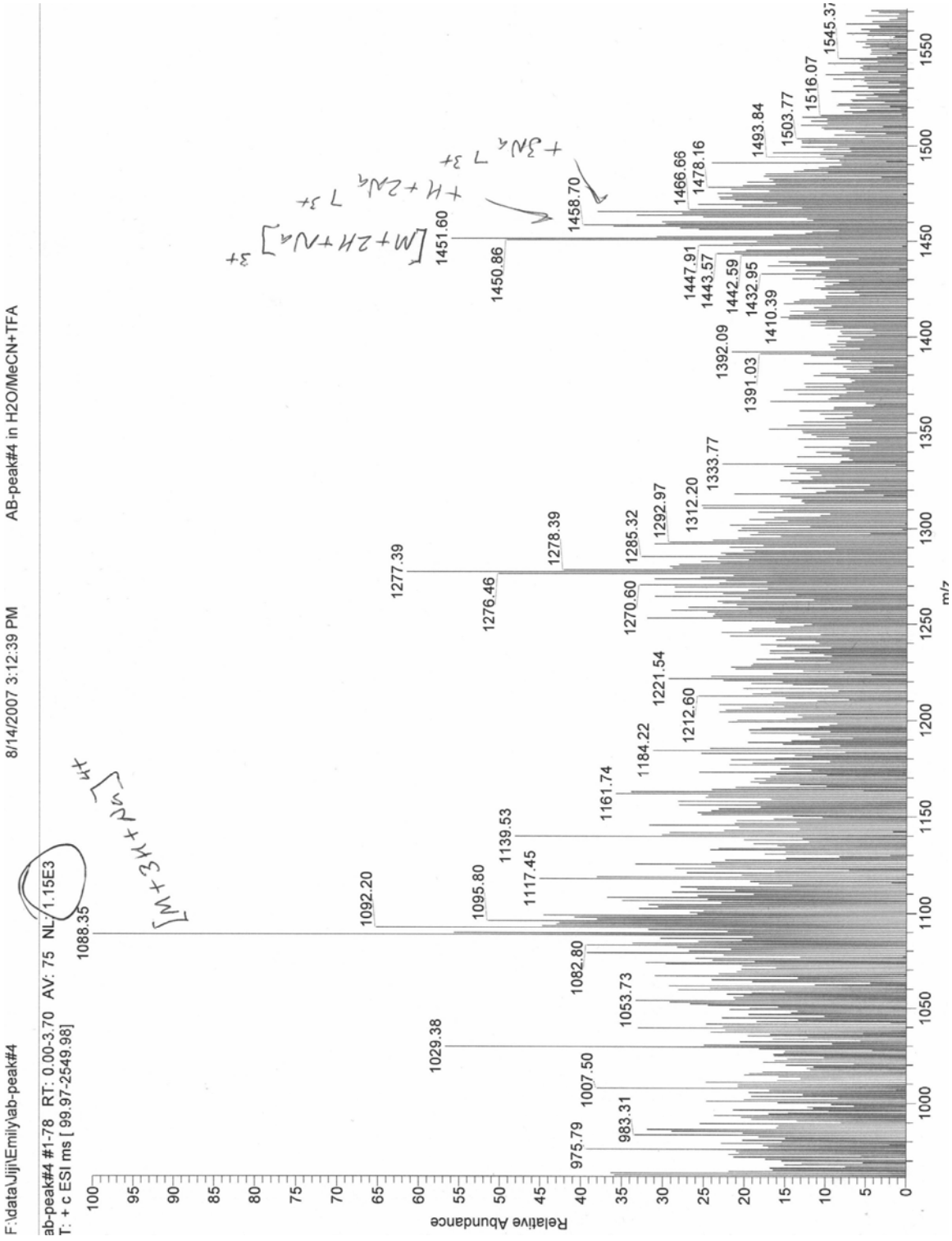

Figure A.2.1 Section of raw MS spectrum for crude Aβ(1-40) purified in 0.1% TFA solvents with peak elution time of 17 minutes.

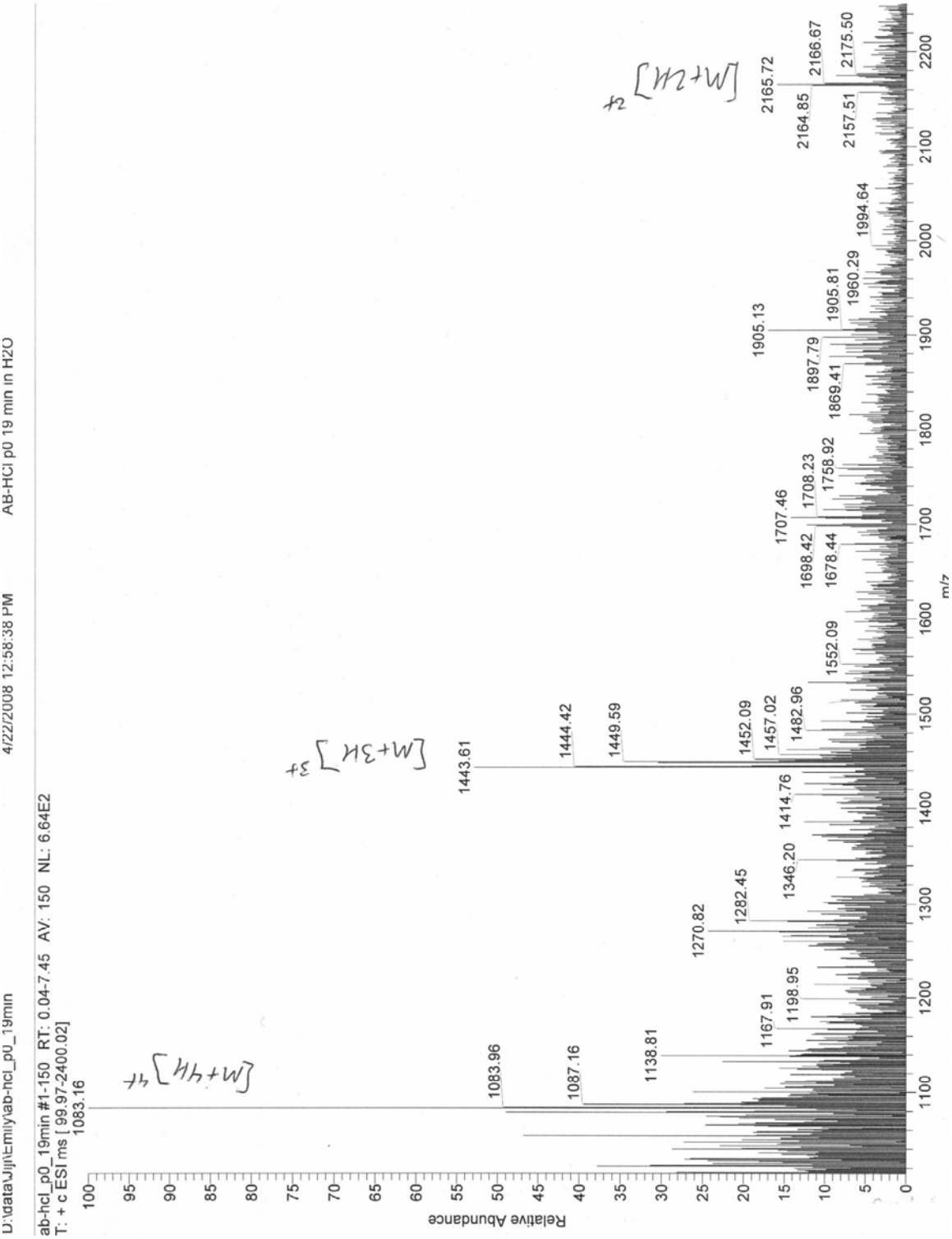

Figure A.2.2 Section of raw MS spectrum for crude Aβ(1-40) purified in 0.1% HCl solvents with peak elution time of 19 minutes.

A.3 MatLab PCR Function

Emily Schmidt
University of Missouri – Columbia
Created May 2007
Filename: PCR.m

```
function [cunkPCR]=PCR(Xconc,Xresp,unk)
%cunkPCR is the new variable created
%Xconc is a matrix of amino acid vs. concentrations in the standards
%Xresp is a matrix of the corresponding absorbance data of the
  standards
%unk is a vector of the response (absorbance data) for the peptide at
%unknown concentration
[I K]=size(Xconc);
n=2;
%number of principle components
[U S V]=svd(Xresp');
%performs singular value decomposition of Xresp matrix
for k=1:K
    b(:,k)=[V(:,1:n)*inv(S(1:n,1:n))*transpose(U(:,1:n))]*Xconc(:,k);
    %determines regression factor (b)
    cunkPCR(:,k)=b(:,k)'*unk;
    %solves for unknown concentration based on calculated regression
      factor
    %and the response (absorbance) of the peptide at unknown
      concentration
end
```

A.4 Molecular Weights and Amino Acid Sequences of Four Peptides

β-Amyloid (1-40)
MW: 4329.8 g/mol
Amino Acid Sequence:
DAE***F***RHDSG***Y***EVHHQKLV***FF***AEDVGSNKGAIIGLMVGGVV

Angiotensin II
MW: 1046.2 g/mol
Amino Acid Sequence: DRV***Y***IHP***F***

Endomorphin I
MW: 610.3 g/mol
Amino Acid Sequence: ***Y***P***WF***

Glucagon (1-29)
MW: 3482.6 g/mol
Amino Acid Sequence: HSQGT***F***TSD***Y***LDSRRAQD***F***VQ***W***LMNT